

## Influence of coronal mass ejections on global electric circuit

C P Anil Kumar\*, C Panneerselvam, K U Nair, K Jeeva, C Selvaraj, S Gurubaran & R Rajaram<sup>1</sup>  
Equatorial Geophysical Research Laboratory, Indian Institute of Geomagnetism, Krishnapuram, Tirunelveli,  
Tamilnadu 627 011, India

<sup>1</sup>Indian Institute of Geomagnetism, New Panvel (W), Navi Mumbai, 410 218, India  
cpanil@iigs.iigm.res.in

Received 20 June 2006; revised 31 May 2007; accepted 29 January 2008

This paper is concerned with the elucidation of flow of particles and field from the sun into the terrestrial system and their subsequent role in Global Electric Circuit (GEC). Many flare associated Coronal Mass Ejections (CMEs) have been studied from ACE satellite data during the last phase of the 23<sup>rd</sup> solar cycle. Such solar ejections consist of hot electrons, protons and helium ions embedded in magnetic fields of various intensities and which travel with velocities greater than supersonic speed towards the earth and breach terrestrial magnetic fields (under favourable conditions) and cause geomagnetic storms. Contemporary data of geoelectrical measurements made at the high latitude Indian Antarctic Research Station, Maitri (70.45°S, 11.44°E) have also been used to investigate the electrical processes during, before and after the above events. The study leads to the conclusion that CMEs enhance the population of the multi-ion plasma species, which paves the way for an increase in the overhead ionospheric electric potential during the onset or even up to the main phase of the magnetic disturbance. The near earth electrical environment is besieged with magnetic disturbance at the high latitude.

**Keywords:** Coronal mass ejections, Atmospheric electricity, Global electric circuit

**PACS No.:** 96.60 ph, 92.60 Pw

### 1 Introduction

The solar origin of geomagnetic disturbances is well accepted, but the exact GEC linkage in magnetosphere-ionosphere-atmosphere system after CMEs is not yet well understood. A lot of effort has been made in the past few centuries to study the influence of solar activity on geoelectric field; it probably may have started even before 1752, with Benjamin Franklin's kite experiments. Contemporary, fair weather atmospheric electric effects were discovered by Lemonnier; the new concept of global atmospheric electric circuit was put forward by Lord Kelvin in 1860. Further research by Kahler and Wilson<sup>1</sup> lead to significant contributions in the realm of geo-electricity. By 1929 a crude picture of Global Electric Circuit (GEC) started emerging; according to this, the ionosphere was considered as a perfect conductor and the earth and the ionosphere formed a spherical capacitor, which shielded the earth from any electric hazard from outer space (i.e. Faraday cage shielding mechanism). This idea may have inhibited further research regarding the influence of solar activity on atmospheric electricity for a short span<sup>2</sup>.

From the beginning of the satellite era<sup>3-6</sup>, and later Wilson<sup>7</sup>, Raina<sup>8</sup>, Tinsley<sup>9</sup>, Kamra *et al.*<sup>10</sup>, Lakhina<sup>11</sup>

and Papitashvili *et al.*<sup>12</sup> used sophisticated techniques and provided valuable information, both experimentally and theoretically, regarding the existence of large-scale electric fields and currents in earth's magnetosphere and ionosphere. Mathematical models of GEC proved that the magnetospheric electric fields can map down unattenuated into middle atmosphere and with attenuation close to the earth's surface. Mathematical models of Hays and Roble<sup>13</sup>, Volland<sup>14</sup> and Tzur *et al.*<sup>15</sup> are notable works in this direction. Later experiments demonstrated the validity of the model and the findings lead to a spurt into the investigations of relationship between the sun and atmospheric electricity. Efforts continue to try to understand this complex relationship.

In this paper, are presented the vertical electrical field ( $E$ ) and air-earth current density ( $J$ ) measurements made near the earth's surface at Maitri, Antarctica during the time of Coronal Mass Ejections associated with major magnetic disturbances, from January to December, 2004. The day-to-day and diurnal variations were statistically removed by the method of Frank *et al.*<sup>16</sup>

The downward air-earth current being delivered to the surface of the high latitude plateau is larger than

the global average. The ice surface is flat and devoid of obstructions and the electrical conductivity of the ice surface is several orders of magnitude over that of air. The surface can be electrically considered as essentially an infinite conducting plane plate at ground potential. Maitri is located in Schirmacher oasis in the Droning Maude Land, east Antarctica (117 m above mean sea level) and is a very good window to geospace. From the last few decades geomagnetic as well as geophysical measurements have been carried out by Indian Institute of Geomagnetism (IIG) at this station. It is expected that continuous measurements of electric field and current, may provide some insight into the problems related to the modulation of GEC by extraterrestrial sources.

## 2 Instrumentation, data and method of analysis

The instrumentation for Maxwell's current experiment is similar to that used earlier<sup>17</sup>. Measurements of wind speed, wind direction, temperature and humidity were collected from Indian Meteorological Department (IMD) observations made at Antarctica. A visual scanning of cloud monitoring was also done during daytime.

For air-earth current measurement a long wire antenna of length 41.5 m and 1.5 mm diameter is mainly employed. The sensor is fixed 2 m above the ground by means of masts that are electrically separated by Teflon rods. The sensor is connected to a duly calibrated electrometer that has very high input impedance, of the order of five mega ohms and permits extremely low input bias current of the order of  $10^{-14}$  A. A buffer stage LM 308 is connected to the electrometer output. The output signals are further filtered by a low pass filter (3 dB) at the point of 12-bit analog to digital conversion. The ADC card is mounted inside a desktop computer. The later set-up is placed inside an experimental hut.

It is supposed that electric field lines are converging and falling straight onto the copper wire and contribution due to convection activity is negligible. The static effective area proposed by

Tammet *et al.*<sup>18</sup> is utilized for computing the conduction current density.

The vertical electric fields were measured with a field mill, facing upward, made of non-magnetic stainless steel. The sensor and rotor plates are of 8.5 cm diameter. The rotor is rotated by an AC motor (220 V, 50 Hz, 1500 rpm) and is grounded with a carbon brush. When the sensor is alternately exposed and shielded from the lines of the field, the surface charge induced on the sensor is a time varying function of the field. Techniques and instrumentation for studying atmospheric electric field including the working principle of field mills are outlined by Datta and Bhattacharya<sup>19</sup>. After a series of analog signal processing within the field mill circuitry the time varying dc output voltage is fed to another channel of the aforesaid data logger.

The Interplanetary Magnetic Field (IMF) data used in the present study was obtained from Space Environment Data Centre, NOAA, USA. The majority of the effects of solar wind variability manifest themselves through geomagnetic storms ( $D_{st}$ ), magnetic substorms ( $AE$ )<sup>20,21</sup> and change of magnetic activity<sup>23</sup> ( $K_p$ ). Geomagnetic storms are believed to cause the largest global atmospheric effects among all the above phenomena.

Presently five major magnetic disturbances at high latitudes have been selected, which were reported to be CMEs during the year 2004 and presented in Table 1. The geomagnetic data used in this investigation were obtained from World Data Centre (WDC), Kyoto University, Japan. In order to account for the mechanism, the authors have correlated time varying IMF ( $B_x$ ,  $B_y$  and  $B_z$ ) component, solar wind velocity ( $V_{sw}$ ) and ion density with different stages of magnetic disturbances.

To take into account the time lag of solar wind from upstream location of Advanced Composition Explorer (ACE) monitoring space craft, the observation times of all the data were reduced to the earth's location by introducing a time shift  $\tau = D/V$

Table 1—Five major magnetic disturbances at high latitudes

Date	Start time	End time	Maximum bulk speed, km/S
11-12 Feb. 2004	0100 hrs UT on 11 <sup>th</sup>	0600 hrs UT on 12 <sup>th</sup>	759
22-24 July 2004	0100 hrs UT on 22 <sup>nd</sup>	0400 hrs UT on 24 <sup>th</sup>	1254
24-30 July 2004	0500 hrs UT on 24 <sup>th</sup>	2200 hrs UT on 30 <sup>th</sup>	1021
29-31 Aug. 2004	1500 hrs UT on 29 <sup>th</sup>	2200 hrs UT on 31 <sup>st</sup>	442
07-14 Nov. 2004	2400 hrs UT on 6 <sup>th</sup>	2400 hrs UT on 14 <sup>th</sup>	784

where  $D$  is line of sight distance between ACE and earth;  $V$  the incoming stream velocity.

### 3 Results and discussions

This section deals with the flare associated CMEs from ACE satellite data during the year 2004. Such solar ejections consist of hot electrons, protons and helium ions embedded in a magnetic field of various intensities that propagate with supersonic velocities. When directed towards the earth they caused geomagnetic disturbances and atmospheric ionic excitation or relativistic electron impact excitation. Conjugate data of atmospheric electrical measurements were analyzed at the aurora oval (after expansion), to investigate the electrical process during, before and after CMEs associated variation in fair weather atmospheric electric field and conduction current near the earth's surface.

Figure 1 depicts a magnetically quiet day, 19 Feb. 2004. There are nine panels in Fig. 1. They are numbered 1'a' to 1'i' from top to bottom. Except one panel all other values are plotted. The top panel 1'a' shows the hourly mean of the vertical electrical field ( $E$ ); 1'b' depicts conduction current density ( $J$ ), and the panels 1'c' to 1'd' illustrate temperature and

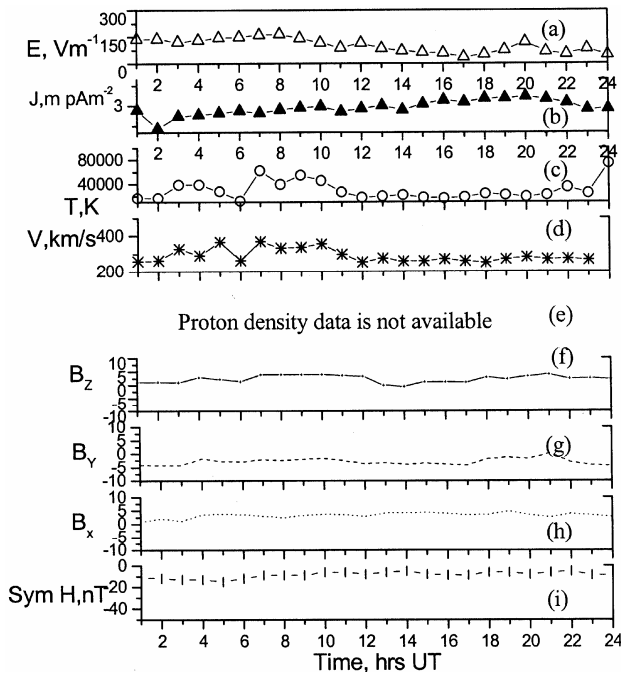


Fig. 1—(a) Hourly means of vertical electrical field ( $E$ ), (b) conduction current density ( $J$ ), (c)-(e) demonstrate the temperature, velocity and proton density, (f) - (h) vertical, azimuthal and radial direction of the in coming IMF and (i) magnetic disturbances observed in terms of Sym-H

speed of the incoming solar wind. Except in Fig. 1, all other cases are coronal transient ejections of coronal material produced either due to solar flare or eruptive prominences, in such cases as the material rapidly moves outwards into the ambient solar wind, the plasma may be compressed and pushed aside by the expanding ejecta.

It is known that the earth does not exist in a vacuum but it is constantly buffeted by the solar wind. As the solar wind flows outside into the interplanetary space, it carries with it a part of the sun's magnetic field, the IMF. It is customary to specify IMF in terms of three mutually perpendicular components with respect to reference axes. Here  $B_x$  is the radial;  $B_y$ , the azimuthal (toward and away from the solar boundary) and  $B_z$ , the vertical (north-south turning) component. The bottom panel component in Fig. 1 shows the magnetic disturbances observed in terms of Sym-H.

Figure 2 represents the measurements of vertical electric field and current during a CME associated magnetic disturbance on 12 Feb. 2004. A substantial increase in current is noted during 0100-0200 hrs UT on 11 February. On the next day, the 12 Feb. 2004, during 0200-0600 hrs UT an increase in both field and

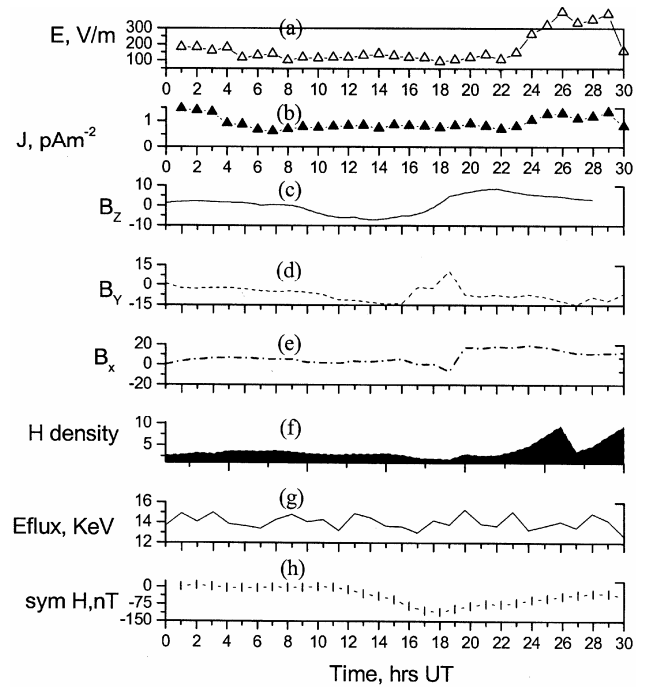


Fig. 2—(a) Shows the hourly means of vertical electrical field ( $E$ ), (b) depicts conduction current density ( $J$ ), (c)-(e) demonstrate the vertical, azimuthal and radial direction of the in coming IMF, (f)-(g) illustrate solar wind parameters proton density and electron flux and (h) shows the magnetic disturbances observed in terms of Sym-H

current was noted in conjunction with an increase in proton density. It is expected that incoming protons may be a cogent agent for modulating the atmospheric electric parameters even under favourable azimuthal direction of IMF.

Figure 3 illustrates the data of global electrical parameters, viz. vertical electric field and current, which were observed during a magnetically disturbed (high  $K_p$ ) day, 22-24 July 2004. The results obtained above provide strong support to the idea that coronal transient ejections influence the  $E$  and  $J$  at high latitudes. The magnetic field near the earth is so strong that it is not easy for the incoming multi-ion plasma to distort the constraint. This implies that, all particles in a dipolar field line must, more or less simultaneously, move together to another field line. Convection of plasma is thus mapped between magnetosphere and ionosphere along the field lines. Hence mapping of the point is very clear, one foot of the magnetic field line is connected to the earth's surface and the other extends into interplanetary space.

Figure 4 represents the measurements of electric field and current in support of the above suggestion.

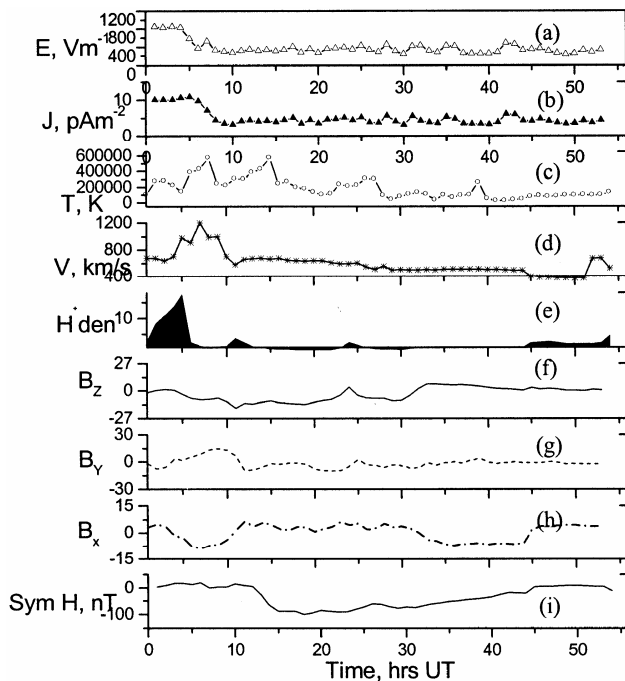


Fig. 3—(a) shows the hourly means of vertical electrical field ( $E$ ), (b) depicts conduction current density ( $J$ ), (c)-(e) illustrate solar wind parameters temperature, velocity and proton density, (f)-(h) demonstrate the vertical, azimuthal and radial direction of the incoming IMF and (i) shows the magnetic disturbances observed in terms of Sym-H

Both the GEC parameters showed an increase with respect to CME associated disturbances during its initial phase span of over 20 hours. The ion accumulations and associated galactic rays, affect the conductivity profile from high to low altitude, and due enhancement in conduction current was expected. This trend was repeated during 2200 hrs UT on 27 July 2004 to 0800 hrs UT on 28 July 2004. This is the reason why CMEs are considered as time invariant enhancing mechanism in the high latitude atmosphere electrical environment, even though the station Maitri has been considered in a rotating frame of reference.

Figure 5 depicts the CME associated magnetic disturbance during 29 - 31 Aug. 2004. The component  $B_z$  turned southward till 2000 hrs UT on 30 Aug. 2004. The solar wind velocity increased during this period. The potential gradient also showed an enhancement during the first day, with an increase in proton density. It would be appropriate and interesting at this stage to state that CMEs constitute a cogent mechanism that modulates the near earth electrical environment.

It has long been known that the development of magnetic disturbances on the earth differs greatly

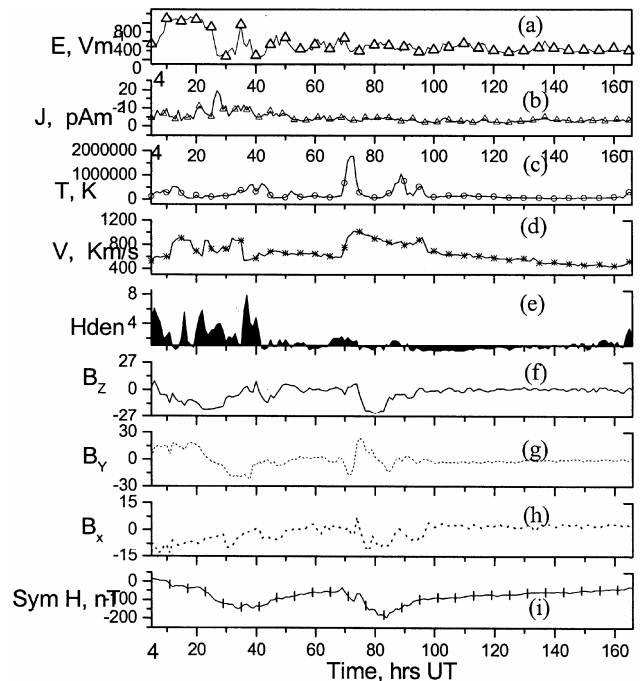


Fig. 4—(a) Shows the hourly means of vertical electrical field ( $E$ ), (b) depicts conduction current density ( $J$ ), and the panels (c)-(e) illustrate solar wind parameters temperature, velocity and proton density, (f)-(h) demonstrate the vertical, azimuthal and radial direction of the incoming IMF and (i) indicates the magnetic disturbances observed in terms of Sym-H

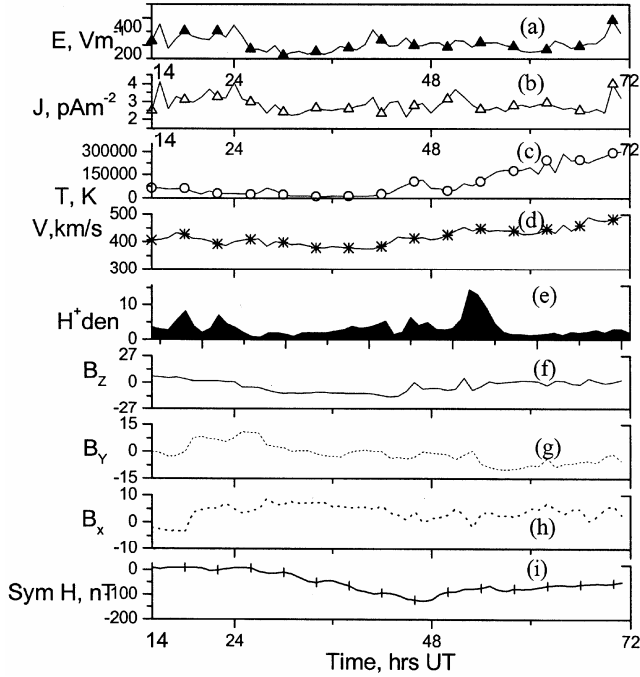


Fig. 5—(a) Depicts the hourly means of vertical electrical field ( $E$ ), (b) depicts conduction current density ( $J$ ), (c)-(e) illustrate solar wind parameters temperature, velocity and proton density, (f)-(h) demonstrate the vertical, azimuthal and radial direction of the in coming IMF and (i) shows the magnetic disturbances observed in terms of Sym-H

from one to another. It is mainly due to the variation in solar wind parameters.

In Fig. 6 has been illustrated a major magnetic disturbance due to CMEs on 7 Nov. 2004. It caused a severe sub-storm too during 11 Nov. 2004. After elimination of the diurnal variation delta ( $E$ ), as in Fig. 7, one can make out that CME associated terrestrial magnetic coupling is an enhancing mechanism to GEC at least in the initial phase, since a high confidence is noted as in Fig. 8 (a). Also, its magnitude of modulation depends on the velocity, direction and density of the incoming solar stream, as in Fig. 8(b), with a correlation coefficient of 0.55. However, the effect of sub-storm on GEC parameters is very small.

It is generally agreed that the major part of the energy transferred from solar wind to the magnetosphere is stored in the ring current. Akasofu<sup>22</sup> theoretically provided a solar wind-magnetosphere energy coupling function ( $\epsilon$ ) and later proved by Kan *et al.*<sup>23</sup>. So, one can expect that the solar wind-magneto dynamo mechanism can be expressed in terms of energy coupling function ( $\epsilon$ ) Anil *et al.*<sup>24</sup>.

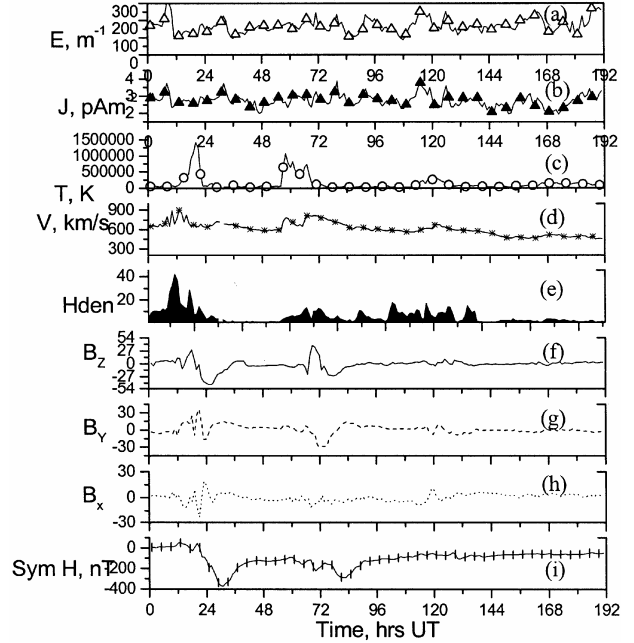


Fig. 6—(a) Shows the hourly means of vertical electrical field ( $E$ ), (b) depicts conduction current density ( $J$ ), (c)-(e) illustrate solar wind parameter temperature, velocity and proton density, (f)-(h) demonstrate the vertical, azimuthal and radial direction of the in coming IMF and (i) shows the magnetic disturbances observed in terms of Sym-H

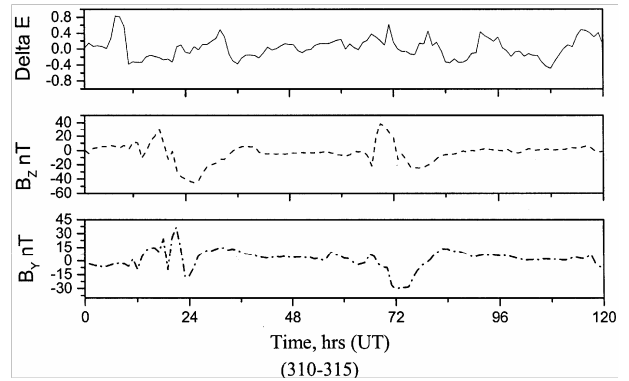


Fig. 7—Signature associated with before, during and after the CME associated variations 7-12 Nov. 2004

Solar wind-magnetosphere dynamo is one of the generators of electric field in GEC. This dynamo results from the flow of solar wind across the open geomagnetic field lines. The magnitude of the field produced by the solar wind-magnetosphere dynamo is given by,  $E = v_{SW} \times B$ . In polar region geomagnetic field line becomes open rather easily when the IMF points southward and map down to the auroral ionosphere and procure a potential difference in the order of 50-120 kV across the polar cap<sup>25</sup>. This dawn-

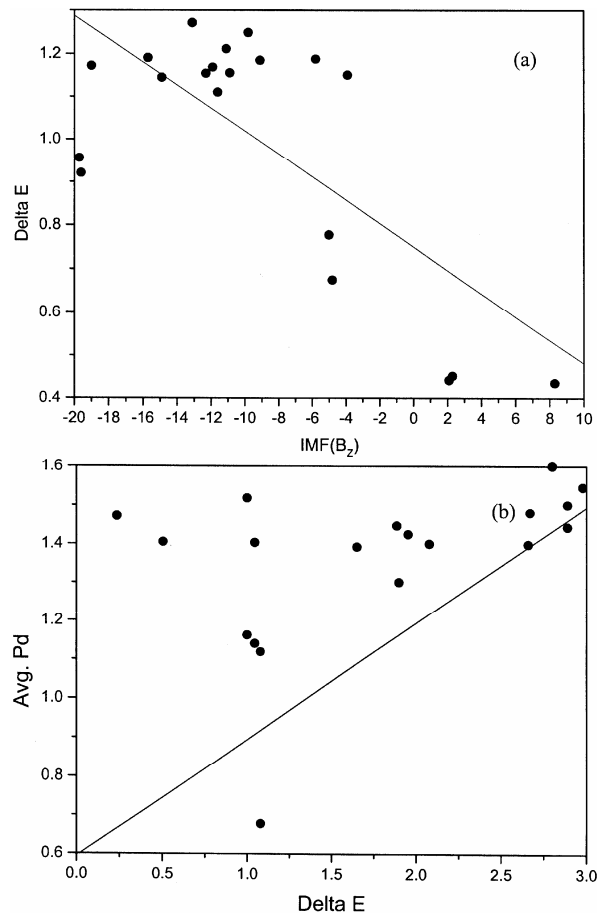


Fig. 8—(a) Negative correlation with IMF ( $B_z$ ) northward component with respect to delta  $E$  and (b) a positive correlation with proton density with respect to delta  $E$

dusk potential difference during magnetically quiet times may not play a dominant role over Maitri (Geomag. Lat.  $67.14^\circ\text{S}$ , Long.  $57.44^\circ\text{E}$ ). But during magnetically disturbed days, plasma convection pattern expands and the station comes under the auroral oval. As a result, potential gradient at this station varies with respect to overhead ionospheric potential. The diurnal variations have been removed by statistical method (it may be due to tropical and subtropical thunderstorm activity) and CME associated GEC signatures are depicted in Fig. 7. Since the satellite data of quiet time magnetosphere-ionosphere convection pattern is not available, the accuracy varies between  $\pm 5$ .

From the foregoing results and discussions it is believed that not only the southward IMF but also the magnitude and velocity of the ejected particles play a crucial role in breaching terrestrial magnetic field and modifying the GEC parameters at high latitudes.

#### 4 Conclusions

Out of 155 fair weather day's data obtained from Indian Antarctic station Maitri during the year 2004, the authors have investigated the effect of near earth electric field and air-earth current density during CMEs associated geomagnetic disturbances of five major selected events. Statistical correlation methods were used to investigate and test associations on, before and after the transient eruptions and associated magnetic disturbances. The study provides evidences of enhancement in the atmospheric electrical potential gradient during onset/ transfusion of charged particle and the position of current sheet with reference to the ecliptic plane (strong during southward component of IMF). Some variations suggest that conditions during magnetically quiet conditions may be totally altered when compared to CME associated disturbances. Understanding the fascinating affect of CMEs associated changes in GEC is a challenge for atmospheric weather studies.

#### Acknowledgement

This GEC project is supported by the Department of Science and Technology, Government of India, New Delhi.

#### References

- 1 Wilson C T R, Investigation on lightning discharges and on the electric field of Thunderstorms, *Phil Trans (UK)*, A221 (1920) 73.
- 2 Raina B N, *Influence of solar activity on atmospheric electricity, Cloud Physics and Atmospheric Electricity*, Vol II, Edited by A K Kamra, 2001, 1080.
- 3 Mozer F S & Serlin R, Magnetospheric electric fields measurements with Balloons, *J Geophys Res (USA)*, 74 (1969) 4739.
- 4 Kasemir H, Atmospheric electric measurements in the Arctic and Antarctic, *Pure Appl Geophys (USA)*, 100 (1972) 70.
- 5 Israel H, *Atmospheric electricity*, Vol II, (Israel Progr. Sci. Translation, Jerusalem), 1973, 113.
- 6 Park C G, Solar magnetic sector effects on the vertical atmospheric electric field at Vostok, Antarctica, *Geophys Res Lett (USA)*, 3 (1976) 475.
- 7 Wilson J M, Interplanetary magnetic field and troposphere circulation, *Weather and climate response to solar variation*, Edited by B M Cormac (Colorado University Press, Boulder, Colorado, USA), 1983, 341.
- 8 Raina B N, Modulation of global electric circuit by extra-terrestrial influences, *Publs Inst Geophys Pol Acad Sci (Poland)*, D-35 (1991) 238.
- 9 Tinsley B A, Solar wind mechanism suggested for weather and climate Changes, *E O S J (USA)* 75 (1994) 369.
- 10 Kamra A K, Murugavel P, Pawar S D & Gopalakrishnan V, Background aerosol concentration derived Physical properties of aerosols at Maitri, *Antarctica* from the atmospheric electric conductivity measurements made over

- the Indian Ocean during INDOEX; *J Geophys Res (USA)*, 106 (2001) 28643.
- 11 Lakhina G S, Electrodynanic coupling between different regions of the Atmosphere. *Curr Sci (India)*, M64 (1993) 660.
  - 12 Papitashvili, V O, Christiansen F & Neubert T, Field-aligned currents during IMF, *Geophys Res Lett (USA)*, 28 (2001) 3055.
  - 13 Hays P B & Roble R G, A quazi-static model of global atmospheric electricity. 1 The lower atmosphere, *J Geophys Res (USA)*, 84 (1979) 3291.
  - 14 Volland H, Mapping of the electric fields of Sq. currents into the lower Atmosphere, *J Geophys Res (USA)*, 77 (1972) 1961.
  - 15 Tzur I, Roble R G & Adams J C, Atmospheric electric fields and currents configurations. *J Geophys Res (USA)*, 90 (1985) 5979.
  - 16 Frank-Kamenetsky A V, Troshichev O A, Burns G B & Papitashvili V O, Variations of atmospheric electric field in the near-pole region related to the interplanetary magnetic field, *J Geophys Res (USA)*, 106 (2001) 179.
  - 17 Panneerselvam C, Nair K U, Jeeva K, Selvaraj C, Gurubaran S & Rajaram R, A comparative study of atmospheric Maxwell current and electric field from a low latitude station, Tirunelveli, *Earth Planet Space (Japan)*, 55 (2003) 697.
  - 18 Tammet H, Israelson S, Knudsen E & Tuomi J J, Effective area of a horizontal long-wire antenna collecting the atmospheric electric vertical current, *J Geophys Res (USA)*, 101 (1996) 29671.
  - 19 Datta T and Bhattacharya A B, Atmospheric electrical field in relation to severe meteorological disturbances, *Indian J Radio Space Phys*, 33 (2004) 373.
  - 20 Belova E, Kirkwod S & Tammet H, The effects of magnetic substorms on near-ground atmospheric current, *Ann Geophys (France)*, 18 (2001) 1623.
  - 21 Arun T, Ajay Dhar, Emperumal K & Pathan B M, IMF B<sub>Y</sub> dependence of the extent of substorm westward electrojet. *J Earth Syst Sci (India)*, 114 (2005) 177.
  - 22 Akasofu S I, Prediction of developments of geomagnetic storms using the solar wind-magnetosphere energy coupling function  $\epsilon$ , *Planet Space Sci (USA)*, 29 (1981)1151.
  - 23 Kan J R, Lee L C & Akasofu S I, The energy coupling function and the power generated by the solarwind–magnetosphere dynamo, *Planet Space Sci (USA)*, 28 (1980) 823.
  - 24 Anil Kumar C P, Panneerselvam C, Nair K U, Jeeva K, Selvaraj C, Gurubaran S & Rajaram R, *Influence of azimuthal and vertical components of IMF on atmospheric electrical parameters at Maitri, Antarctica*, National Space Science Syposium, 65, 2006.
  - 25 Tinsley B A, Correlations of atmospheric dynamics with solar wind-induced changes of air-earth current density inter cloud tops, *J Geophys Res (USA)*, 101 (1996) 29701.